

## GEOLOGY

# The Lower–Middle Riphean Boundary in the Southern Urals: New Isotopic U–Pb (SHRIMP II) Constraints

Yu. L. Ronkin<sup>a</sup>, Corresponding Member of the RAS A. V. Maslov<sup>a</sup>,  
A. P. Kazak<sup>a</sup>, D. I. Matukov<sup>b</sup>, and O. P. Lepikhina<sup>a</sup>

Received February 6, 2007

DOI: 10.1134/S1028334X07060025

In the general Precambrian stratigraphic scale of the former USSR approved at the 2nd All-Russia meeting on general problems of Precambrian stratigraphy (Ufa, 1990), the Riphean representing the largest Upper Proterozoic subdivision comprises three chronostratigraphic units—the Lower Riphean (Burzyanian), Middle Riphean (Yurmatinian), and Upper Riphean (Karatavian)—with the lower isotopic boundaries at  $1650 \pm 50$ ,  $1350 \pm 20$ , and  $1000 \pm 50$  Ma, respectively [1]. The Riphean–Vendian boundary is placed at  $650 \pm 20$  Ma.

Since that time, the stratigraphic position of some of these boundaries has changed. For example, based on Pb–Pb dating of limestones from the Neruen Formation (Lakhanda Group, Yudoma–Maya region) and carbonate rocks from the Sukhaya Tunguska Formation (Turukhansk area), the Yurmatinian–Karatavian boundary is now drawn at  $1030 \pm 30$  Ma [2]. The Riphean–Vendian boundary is now substantially younger (600 Ma) [3]. Only the Burzyanian–Yurmatinian boundary is still accepted in its former position at 1350 Ma [3].

In the stratotype region corresponding to the Bashkir Meganticlinorium of the Southern Urals, the age of the Lower–Middle Riphean is based on isotopic Rb–Sr (bulk samples) and U–Pb (zircons) isotopic dating of dacites and rhyodacites from the Mashak Formation ( $t_{\text{Rb-Sr}} = 1346 \pm 41$  Ma,  $t_{\text{U-Pb}} = 1350 \pm 30$  Ma) that occurs at the base of the Yurmata Group, rapakivi granites, and associated rocks from the Berdyaush Massif ( $t_{\text{Rb-Sr}} = 1348 \pm 13$  Ma,  $t_{\text{U-Pb}} = 1354 \pm 20$  Ma). At this level ( $1350 \pm 10$  Ma), it is accepted “with a high degree of confidence” in some works [4, p. 132; 5, p. 144].

Assessing from the present-day standpoint, the reliability of previous isotopic age estimates used for substantiation of the Burzyanian–Yurmatinian boundary,

and the expediency of new investigations, the following points should be noted.

The methodology and resolution of Rb–Sr and U–Pb methods applied in the early 1980s were characterized by the corresponding approaches to graphic interpretations of experimental data and the possibilities of the instrumental–analytical techniques of that time.

The behavior of the Rb–Sr isotopic system in the main rock varieties from the Berdyaush Massif and subvolcanics from the Mashak Formation is significantly complicated by metasomatic transformations. For example, the examined samples of dacites and rhyodacites from the Mashak Formation appeared to be variably sericitized, silicified, and chloritized, which led to substantial elevation in K and Rb and, partly, Ca and depletion in Na and Sr. Rapakivi granites and associated rocks of the Berdyaush Massif are characterized by notable K-feldspathization and albitization that lead to age discordance of the Rb–Sr system and hamper the choice of samples for isochronic dating.

The U–Pb data available for zircons from volcanics of the Mashak Formation and igneous rocks of the Berdyaush Massif [4] were approximated using the “simple” method of least squares that leaves aside errors and their correlation along both coordinate axes. The recalculation of U–Pb digital data using the present-day processing algorithm [6] reveals significantly larger MSWD values that determine the degree of consistence of obtained data of the isochron model (for example, the MSDW value for zircons from quartzose syenite-diorites and granites of the Berdyaush Massif is 474 and 28, respectively). Moreover, samples up to  $n$  mg in weight (hundreds of thousands of individual zircon grains) were dated by the “classical” U–Pb method. It is clear that even after selecting zircons under the microscope, the age values obtained for such grain populations are characterized by substantial averaging, which cannot be described in the framework of sufficiently unitary graphic models applied for interpretation of U–Pb isotopic data.

Finally, the U–Pb (ID-TIMS) dating of single zircon grains from nepheline syenites of the Berdyaush Massif

<sup>a</sup> Zavaritskii Institute of Geology and Geochemistry, Ural Division, Russian Academy of Sciences, Pochtovyi per. 7, Yekaterinburg, 620219 Russia; e-mail: ronkin@r66.ru

<sup>b</sup> Karpinskii All-Russia Research Institute of Geology, Srednii pr. 74, St. Petersburg, 199106 Russia

[7] yielded  $1368.4 \pm 6.2$  Ma, which is significantly older than the previously reported values (1086 and 1302 Ma) [4]. A close (within limits of the observed accuracy) value of  $1373 \pm 21$  Ma was obtained for nine zircon crystals from nepheline syenites by the U–Pb (SHRIMP II) method [8]. According to most researchers, nepheline syenites formed at the terminal stage of development of the Berdyaush Massif. Therefore, dating of zircons from gabbro and rapakivi granites using the state-of-art analytical technique seems essential for specifying the Lower–Middle Riphean boundary and stratigraphic position of volcanic rocks of the Mashak Formation.

The Berdyaush Massif of rapakivi granites is located in the northeastern part of the Bashkir Meganticlinorium near the synonymous station of the South Ural Railway. It is approximately 35 km<sup>2</sup> in size and characterized by more or less prominent concentric zoning: granites and granosyenites developed in the outer zone give way to syenite-diorites and syenites toward the central part of the massif, where alkaline and nepheline syenites are widespread as dikes and veins (products of the late stage of the Berdyaush Massif formation). In addition, the massif also includes relatively small melanocratic rocks (autoliths and xenoliths) and separate gabbro and gabbro-dolerite outcrops. According to V.I. Petrov, B.N. Punegov, and A.S. Shalaginov who investigated the Satka area at scale 1 : 50 000 in 1990, granites occupy a substantially smaller area than was considered by A.N. Zavaritskii, while coarse-grained and pegmatoid rapakivi syenites and gabbro with hybrid syenite-diorites are more widespread. It was also shown that hybrid porphyric syenite-diorites with stratiform bodies of gabbroids, monzonitic gabbro, monzonitic gabbrodiorites, and monzonites occupy a significant part of the massif. Petrov et al. did not find any active contacts of the massif with the Bakal Formation (Burzyan Group), although it was previously considered that rapakivi granites intrude the Satka Formation and metamorphose the Bakal Formation [4, 5, 9]. Taking into consideration present-day petrogenetic constraints based on trace elements, the Berdyaush rapakivi correspond to A-type granites and fall into the field of intraplate rocks in the tectonomagmatic classification [11].

The Mashak Formation (2500–3000 m thick) corresponds to the basal part of the Middle Riphean Yurmata Group (Fig. 1) and consists of sedimentary, volcanosedimentary, and igneous rocks. It is confined to structures controlled by the Zyuratkul deep fault and is traced for nearly 250 km in the meridional direction [10]. The proportions between terrigenous and igneous rocks in this formation are highly variable in the latitudinal and meridional directions. Conglomerates at the base of the Mashak Formation contain rounded pebbles and boulders of sandstones and quartzite sandstones from the underlying Lower Riphean Yushino Formation. Igneous rocks are widespread in the formation as dolerite sills frequently characterized in many places by

“hot” contacts with host sedimentary rocks (S.G. Kovalev, private communication, 2007) and by subvolcanic dacite and rhyodacite bodies. They are metamorphosed up to greenschist facies, but relatively well-preserved microtextures are retained.

Samples collected during field work between 1998 and 2006 were used for U–Pb isotopic dating. Zircons were extracted from gabbro and rapakivi granites of the Berdyaush Massif and from dacites of the Mashak Formation using the traditional procedure. After crushing the initial samples, heavy minerals were separated with the help of sieving, a concentration table, an isodynamic magnetic separator, and heavy liquids. Finally, appropriate zircon grains were hand-picked under a binocular microscope.

Zircons from gabbro are represented by large (>350 μm) fragments (GA2) and euhedral (GA1) white and pink crystals. The U and Th contents are relatively low (198–368 and 200–355 ppm, respectively). Cathodoluminescence (CL) images are characterized by practically homogenous fluorescence (Fig. 2).

Zircons from rapakivi granites are large (up to 300 μm) pink crystals with distinct (GR1.1, GR2.1, GR8.1, GR11.1) to less distinct (GR3.1) euhedral patterns. Some zircons demonstrate apparent rhythmic zoning (GR1, BRD2.1). The central parts of some crystals are characterized by both relatively low (GR1.1–GR3.1, GR7.1) and high (GR6.1) intensities of the fluorescence. The CL pattern can be homogenous (GR7.1) or relatively heterogeneous (BRD6.1, GR9.1, GR11.1) owing to complex block-shaped (GR6.1) and/or mosaic (GR8.1, GR9.1, GR11.1, BRD9) structures. Some grains enclose inclusions of highly variable compositions and shapes (GR6.1).

In general, mineralogical peculiarities established in Berdyaush zircons imply that their relative mineralogical–geochemical heterogeneity increases from gabbro to granites, reflecting the complicated evolution of the massif.

Zircons from dacites of the Mashak Formation are also highly variable in their appearance and internal structure. They occur as both transparent (14.3.1, 14.5.1) and hazy (7.2.1) species. The degree of idiomorphism ranges from perfect (7.2.1, 14.5.1, 14.8.1) to less distinct (7.7.1) varieties. Asymmetric crystals with overgrowths (14.4.1) are also found. One can see numerous inclusions with different degrees of filling. They are characterized by a wide range of size and orientation (7.7.1, 14.5.1, 14.7.1). Some crystals bear signs of crushing (7.2.1).

The selected specimens were fixed together with standards 91 500 and TEMORA by the Epofix resin on a disc (25 mm across), which was polished until crystals appeared at the surface. Further, using a CamScan MX2500 scanning electron microscope equipped with a CLI/QUA2 (Bentham) cathodoluminescence equipment, we obtained CL images of zircons, which made it possible to select areas for local U–Pb dating most

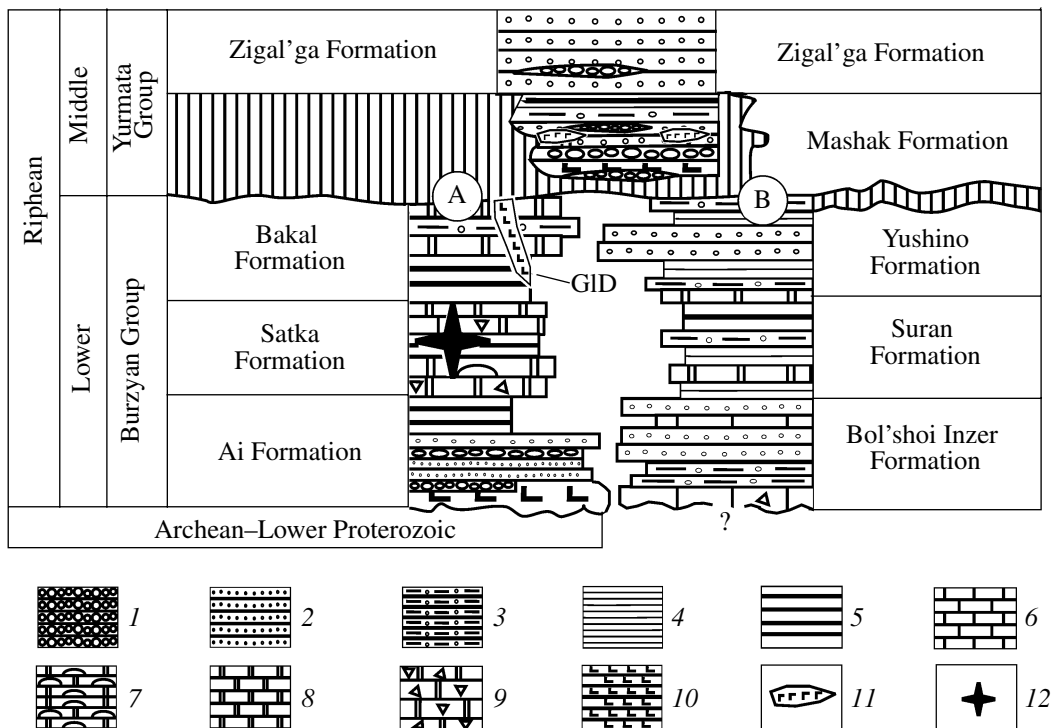


**Fig. 1.** Fragment of the Riphean reference section in the Bashkir Meganticlinorium and position of the Berdyaush rapakivi granite massif and Main dike (MD) of the Bakal ore field in the massif. (1) Conglomerate; (2) sandstone; (3) siltstone; (4) shale and argillite; (5) low-carbonaceous shale; (6) limestone; (7) stromatolitic limestone; (8) dolomite; (9) platy-clastic carbonate syndimentary breccia; (10) igneous rocks (dolerite, metabasalt, dacite, rhyolite–dacite); (11) acid igneous rocks (dacite, rhyolite–dacite); (12) rapakivi granites and associated rocks of the Berdyaush Massif. (A) Northeastern areas of the Bashkir Meganticlinorium; (B) central areas of the Bashkir Meganticlinorium.

appropriate from the standpoint of the experimental methodology. The dating was performed using a SHRIMP II high-resolution secondary ion microprobe (Central Research Institute, St. Petersburg).

In total, the U–Th–Pb isotopic composition was studied at 30 points in 2 crystals from gabbro, 18 grains from rapakivi granites, and 8 grains from dacites of the Mashak Formation (table). The largest size of the examined ellipsoid spot was approximately 30  $\mu\text{m}$ .

Experimental data obtained for zircons from gabbro demonstrate in the  $^{207}\text{Pb}/^{235}\text{U}$ – $^{208}\text{Pb}/^{238}\text{U}$  plot relatively insignificant discordance for three “shots” (Ga2.1–GA2.3) in crystal GA1. In contrast, the data point of zircon GA1 show a discordance of 11%. Taking into consideration close values of U–Pb data obtained for GA2 zircons, the SHRIMP II values were considered as concordant values defining the age of  $1386 \pm 9.8$  Ma ( $\pm 1\sigma$ , MSWD = 0.053, probability 0.89). Approximation of U–Pb data for both crystals (GA1 and GA2) suggests that the upper intercept of concordia with discordia corresponds to  $1389 \pm 28$  Ma with MSWD = 0.73 and practically two times lower probability (0.48).

In the Ahrens–Wetherill plot, the U–Pb data points obtained for zircons from rapakivi granites demonstrate low discordance (from –2.9 to 1.5). They are localized

in the area of 1370 Ma with some overlapping. Data points corresponding to BRD2.1 and BRD9.2 are located above all other points (Fig. 3) and define an older age. For example, the “crater” BRD2.1 representing the crystal core yields an age of  $1416 \pm 21$  Ma ( $\pm 2\sigma$ , MSWD = 0.008, probability 0.93). The “crater” BRD9.2 localized in the most heterogeneous (according to the cathodoluminescence data) part of the crystal provides an older age of  $1423 \pm 16$  Ma ( $\pm 2\sigma$ , MSWD = 1.5, probability 0.21). However, analysis BRD9.1 made in the peripheral part of the crystal yielded a substantially younger age of  $1363 \pm 12$  Ma ( $\pm 2\sigma$ , MSWD = 0.013, probability 0.91). The older ages obtained for craters BRD2.1 and BRD9.2 are probably related to the following fact. The CL data indicate the presence of inherited “cores” in zircons BRD2 and BRD9 from rapakivi granites. Like zircons from gabbro (GA1, GA2), the cores are characterized by similar age values and low U concentrations.

The formal approximation of the entire data array in the concordia plot reveals a relatively higher MSWD value (2.9). Omission of data points of craters BRD2.1 and BRD9.2 from the calculation yields the concordance age of  $1374 \pm 5.7$  Ma (confidence level 95%, MSWD = 1.9, probability 0.17). The further decrease of the MSWD value to 0.5 is caused by omission of U–

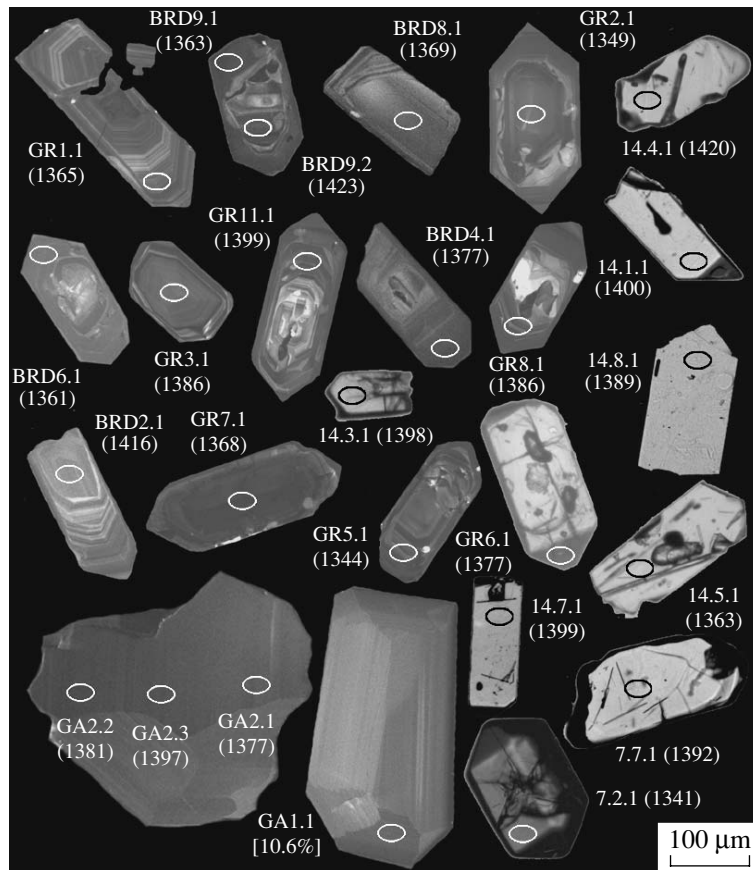


**Fig. 2.** Cathodoluminescence and optical (in transmitted light) images of single individual zircon crystals from gabbro (GA), rapakivi granites of the Berdyaush Massif (GR, BRD), and dacites of the Mashak Formation (others). The ellipses demonstrate localization of craters up to 30  $\mu\text{m}$  across and up to 3–4  $\mu\text{m}$  deep formed at the surface of crystals under influence of the SHRIMP II primary oxygen beam. Numerals in parentheses designate age (Ma) calculated in  $^{207}\text{Pb}/^{235}\text{U}$ – $^{206}\text{Pb}/^{238}\text{U}$  coordinates.

Pb data related to BRD3.1 from the data array, resulting in the concordance age of  $1370.0 \pm 4.6$  ( $\pm 2\sigma_0$ ) and the highest correlation probability (0.48) relative to other versions of calculation.

Analogous calculations based on the U–Pb zircon dating for dacites of the Mashak Formation (Fig. 4) yield a concordant cluster ( $N = 8$ ) with an age of  $1370 \pm 16$  Ma (confidence level 95%, MSWD = 0.73, probability 0.39).

The obtained age value coincides (within the limits of the observed accuracy) with our previous U–Pb age estimates obtained for zircons from nepheline syenite porphyries ( $1368.4 \pm 6.2$  Ma, ID-TIMS [7];  $1373 \pm 21$  Ma, SHRIMP II [8]) and quartz syenite porphyries ( $1372 \pm 12$  Ma, SHRIMP II [11]). This fact confirms that the Berdyaush Massif is older than was accepted previously [4].

Combined with data on the age of gabbro, granite gneisses, and granites from the Kusinsk–Kopan Complex (LA ICP-MS data: Kusinsk Massif,  $1388 \pm 63$  Ma, Sm–Nd method [12]; Kopan Massif,  $1385 \pm 25$  Ma; Ryabinov Massif,  $1386 \pm 34$  Ma; Gubensk

Massif, Ma,  $1330 \pm 16$  and  $1330 \pm 27$  Ma [13]<sup>1</sup> localized in the Lower–Middle Riphean rocks of the north-eastern Bashkir Meganticlinorium, the materials mentioned above indicate that the “Mashak riftogenic event” has a more complicated evolution than was previously assumed [11]. With account for the accuracy of modern isotopic datings, its duration may be estimated at approximately 18–20 Ma (without the consideration of LA ICP-MS data [13]). This is relatively consistent with the evolution duration of model intracontinental rift structures, such as the Late Cenozoic rift region of Ethiopia (~30 Ma) or Late–Middle Riphean Mid-Continent rift system (~20 Ma) [14]. The Lower–Middle Riphean boundary in the Bashkir Meganticlinorium is defined by two principal groups of isotopic–geochronological data: (i) U–Pb zircon datings for dacites of the Mashak Formation ( $1370 \pm 16$  Ma); nepheline syenites ( $1368.4 \pm 6.2$  Ma and  $1373 \pm 21$  Ma), quartz syenite porphyres ( $1372 \pm 12$  Ma), and gabbro ( $1389 \pm 28$  Ma)

<sup>1</sup> Unfortunately, based on materials presented in this work, it is impossible to estimate the validity of U–Pb ages obtained by laser ablation and quadrupole mass spectrometer (Elan5000) measurements.

U–Pb SHRIMP II data obtained for zircons from gabbro and rapakivi granites of the Berdyaush Massif and dacites of the Mashak Formation

Crystal, crater	$^{206}\text{Pb}_c$ , %	U	Th	$\frac{^{232}\text{Th}}{^{238}\text{U}}$	(1)	(1)	(1)	<i>Rho</i>	Age, Ma ( $\pm 2\sigma$ )	MSWD	<i>P</i>	<i>D</i> , %
		ppm			$\frac{^{207}\text{Pb}^*}{^{206}\text{Pb}}$ ( $\pm\%$ )	$\frac{^{207}\text{Pb}^*}{^{235}\text{U}}$ ( $\pm\%$ )	$\frac{^{206}\text{Pb}^*}{^{238}\text{U}}$ ( $\pm\%$ )					
Zircons from gabbro of the Berdyaush Massif												
GA1.1	0.10	205	200	1.01	0.0881 (2.6)	2.602 (2.5)	0.2143 (2.1)	0.82	Discord	13	0.00	10.6
GA2.1	0.11	368	355	0.99	0.0869 (2.6)	2.881 (2.6)	0.2404 (2.0)	0.77	1377 (39)	0.55	0.46	–2.2
GA2.2	0.08	198	207	1.08	0.0881 (2.4)	2.890 (2.4)	0.2380 (2.0)	0.87	1381 (35)	0.056	0.81	0.6
GA2.3	0.09	288	289	1.03	0.0889 (2.3)	2.943 (2.2)	0.2400 (2.0)	0.89	1397 (30)	0.25	0.62	1.2
Zircons from rapakivi granites of the Berdyaush Massif												
GR5.1	2.36	355	571	1.66	0.0859 (2.5)	2.761 (2.5)	0.2331 (2.0)	0.81	1344 (37)	0.16	0.69	–1.1
GR2.1	0.14	538	732	1.41	0.0860 (2.0)	2.819 (2.1)	0.2377 (1.9)	0.93	1349 (26)	1.8	0.18	–2.6
GR7.1	0.05	1197	1494	1.29	0.0873 (2.0)	2.852 (2.0)	0.2369 (1.9)	0.97	1368 (18)	0.016	0.90	–0.2
GR1.1	0.07	529	359	0.70	0.0869 (2.0)	2.867 (2.1)	0.2393 (1.9)	0.93	1365 (26)	0.84	0.36	–1.8
GR8.1	0.16	432	285	0.68	0.0880 (2.2)	2.931 (2.1)	0.2416 (2.0)	0.91	1386 (27)	0.16	0.69	–0.9
GR3.1	0.03	312	271	0.90	0.0878 (2.2)	2.936 (2.2)	0.2425 (2.0)	0.90	1386 (29)	0.46	0.50	–1.5
GR6.1	0.08	621	451	0.75	0.0873 (2.0)	2.942 (2.1)	0.2443 (1.9)	0.94	1377 (25)	2.4	0.12	–2.9
GR11.1	0.05	778	759	1.01	0.0885 (2.0)	3.018 (2.0)	0.2472 (1.9)	0.96	1399 (20)	1.3	0.26	–2.1
BRD6.1	0.06	849	475	0.58	0.0862 (1.1)	2.800 (1.1)	0.2356 (0.6)	0.53	1361 (14)	1.18	0.28	–1.6
BRD7.1	0.07	703	576	0.85	0.0868 (1.5)	2.829 (1.4)	0.2365 (1.0)	0.67	1365 (20)	0.31	0.58	–1.0
BRD9.1	–	831	348	0.43	0.0872 (1.3)	2.833 (1.3)	0.2355 (0.5)	0.40	1363 (12)	0.013	0.91	0.2
BRD1.1	0.00	879	897	1.05	0.0870 (1.0)	2.842 (1.1)	0.2369 (0.5)	0.49	1370 (12)	0.25	0.62	–0.7
BRD8.1	0.25	369	331	0.93	0.0877 (2.7)	2.860 (2.7)	0.2365 (0.8)	0.30	1369 (19)	0.023	0.88	0.6
BRD4.1	0.10	1098	552	0.52	0.0879 (1.1)	2.887 (1.1)	0.2381 (0.5)	0.44	1377 (12)	0.047	0.83	0.3
BRD5.1	0.14	491	330	0.69	0.0885 (1.7)	2.897 (1.6)	0.2374 (0.8)	0.47	1376 (18)	0.48	0.49	1.5
BRD3.1	0.05	1183	903	0.79	0.0883 (1.0)	2.957 (0.9)	0.2429 (0.5)	0.50	1400 (11)	0.6	0.44	–0.9
BRD9.2	0.04	586	378	0.67	0.0888 (1.3)	3.035 (1.3)	0.2479 (0.7)	0.55	1423 (16)	1.5	0.21	–2.0
BRD2.1	0.11	299	312	1.08	0.0897 (2.0)	3.037 (1.9)	0.2456 (0.9)	0.46	1416 (21)	0.008	0.93	0.2
Zircons form dacites of the Mashak Formation												
7.2.1	0.01	841	1231	1.51	0.0867 (1.2)	2.758 (1.3)	0.2307 (0.8)	0.65	1341 (18)	0.56	0.45	1.2
14.5.1	0.09	321	557	1.79	0.0860 (1.9)	2.800 (1.9)	0.2362 (1.0)	0.54	1363 (23)	0.79	0.37	–2.1
14.7.1	0.65	82	165	2.07	0.0860 (4.3)	2.889 (4.1)	0.2436 (1.7)	0.40	1399 (41)	0.79	0.37	–4.8
7.7.1	0.34	79	136	1.79	0.0878 (3.7)	2.924 (3.7)	0.2414 (1.7)	0.46	1392 (40)	0.049	0.82	–1.1
14.1.1	0.14	48	53	1.15	0.0871 (4.2)	2.929 (4.1)	0.2438 (2.1)	0.50	1400 (49)	0.34	0.56	–3.1
14.4.1	0.71	66	87	1.36	0.0870 (4.9)	2.966 (5.0)	0.2473 (1.8)	0.37	1420 (44)	0.5	0.48	–4.5
14.8.1	0.45	65	91	1.45	0.0896 (5.1)	2.966 (5.0)	0.2400 (1.9)	0.37	1389 (0.1)	0.74	0.11	2.2
14.3.1	0.31	153	168	1.13	0.0891 (2.7)	2.972 (2.8)	0.2419 (1.3)	0.48	1398 (31)	0.04	0.84	0.7

Note: Accuracy is  $\pm 1\sigma$ ; ( $\text{Pb}_c$ ,  $\text{Pb}^*$ ) total and radiogenic lead, respectively. Calibration error relative to standards is 0.8% [1]. Correction was performed using  $^{204}\text{Pb}$ . (*D*) discordia,  $100 \cdot (1 - \text{age } ^{206}\text{Pb}^*/^{238}\text{U}) / (\text{age } ^{207}\text{Pb}^*/^{206}\text{Pb})$ . (*Rho*) correlation coefficient of ratios  $^{207}\text{Pb}^*/^{208}\text{Pb}$  and  $^{206}\text{Pb}^*/^{238}\text{U}$ . Age calculated in coordinates  $^{207}\text{Pb}^*/^{238}\text{U}$ – $^{206}\text{Pb}^*/^{235}\text{U}$ . (*P*) Correlation probability. (*D*) Discordant position of the data point in the plot with concordia. More detailed description of the SHRIMP II method of U–Th–Pb ratio measurements is given in [8]. Processing of experimental U–Th–Pb data and compilation of plots with concordia were performed using the ISOPLOT/Ex program [6].

of the Berdyaush Massif; the Sm–Nd mineral isochron of Berdyaush rapakivi granites ( $1371.3 \pm 26$  Ma); (ii) U–Pb datings of dolerites from the Main dike of the

Bakal ore field ( $1385.3 \pm 1.4$  Ma, based on baddeleyite [15]). The dike intrudes and metamorphoses sedimentary rocks of the Bakal Formation (Burzyan Group) but

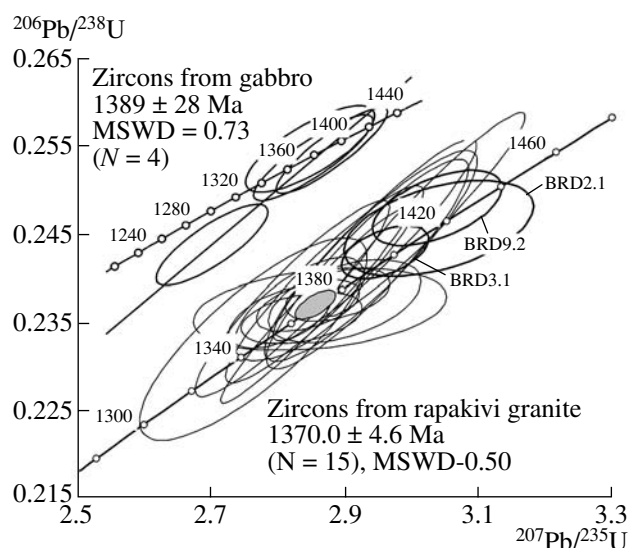


**Fig. 3.** U–Pb SHRIMP II data on zircons from gabbro and rapakivi granites of the Berdyash Massif.

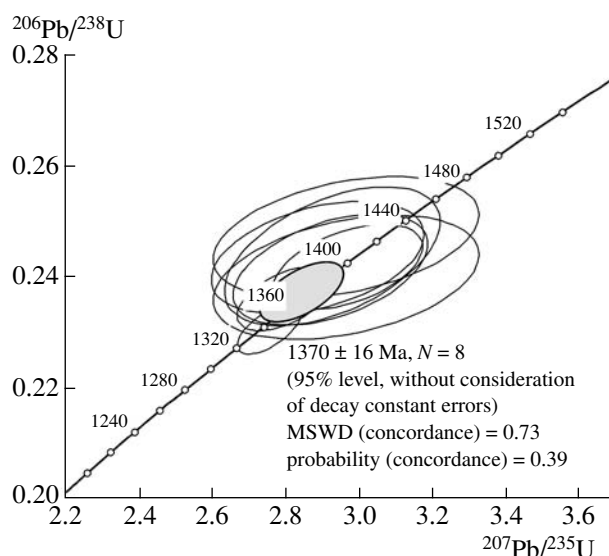


**Fig. 4.** U–Pb SHRIMP II data on zircons from dacites of the Mashak Formation.

does not alter quartzitic sandstones and erosion shales of the Zigal'ga Formation (Upper Riphean Yurmata Group) [10].

Thus, we can conclude that the Lower–Middle Riphean boundary in the stratotype region should be placed within the interval of 1370–1385 Ma.

#### ACKNOWLEDGMENTS

This work was carried out within the framework of Program 8 of the Division of Earth Sciences of the Russian Academy of Sciences “Isotopic Systems and Isotopic Fractionation in Natural Processes.”

#### REFERENCES

1. M. Semikhatov, K. A. Shurkin, E. M. Aksenov, et al., *Izv. AN SSSR. Ser. Geol.*, No. 8, 3 (1991).
2. M. A. Semikhatov, G. V. Ovchinnikova, I. M. Gorokhov, et al., *Dokl. Earth Sci.* **372**, 625 (2000) [*Dokl. Akad. Nauk* **372**, 216 (2000)].
3. *Stratigraphic Code of Russia* (VSEGEI, St. Petersburg, 2006) [in Russian].
4. A. A. Krasnobaev, *Zircon as an Indicator of Geological Processes* (Nauka, Moscow, 1986) [in Russian].
5. *The Lower Riphean of the Southern Urals*, Ed. by M.A. Semikhatov (Nauka, Moscow, 1989) [in Russian].
6. K. R. Ludwig, *Isoplot/Ex ver. 2.49* (Berkley Geochronology Center Spec. Publ., No. 1, 2001).
7. S. Cindern, Yu. L. Ronkin, W. Kramm, et al., in *Isotopic Geochronology in Solving Problems of Geodynamics and Ore Genesis. Abstracts of the All-Russia Meeting (IGGD RAN, St. Petersburg, 2003)*, pp. 461–465 [in Russian].
8. Yu. L. Ronkin, D. I. Matukov, S. L. Presnyakov, et al., *Litosfera*, No. 1, 135 (2005).
9. *Stratotype of the Riphean. Stratigraphy. Geochronology*, Ed. by B.M. Keller and N.M. Chumakov (Nauka, Moscow, 1983) [in Russian].
10. A. V. Maslov, M. T. Krupenin, E. Z. Gareev, and L. V. Anfimov, *The Riphean on the Western Slope of the Southern Urals (Classical Section, Sedimentogenesis, Lithogenesis, Minerageny and Natural Geological Monuments)* (IG KNTs UrO RAN, Yekaterinburg, 2001), Vol. 1 [in Russian].
11. Yu. L. Ronkin, A. V. Maslov, D. I. Matukov, et al., in *Structure, Geodynamics, and Mineragenic Processes in the Lithosphere. Abstracts* (IG KNTs UrO RAN, Syktyvkar, 2005), pp. 305–307 [in Russian].
12. Y. Ronkin, V. Kholodov, O. Lepikhina, et al., *J. Miner.* **18** (1), 112 (2006).
13. A. V. Krasnobaev, G. B. Fershtater, F. Bea, and P. Montero, in *Yearbook-2005* (IGG KNTs UrO RAN, Yekaterinburg, 2001), pp. 300–303 [in Russian].
14. *Sedimentary Basins: Research Methodology, Structure, and Evolution*, Ed. by Yu.G. Leonov and Yu.A. Volozh (Nauch. Mir, Moscow, 2004) [in Russian].
15. R. E. Ernst, V. Rease, V. N. Puchkov, et al., in *Collection of Geological Papers* (IG KNTs UrO RAN, Ufa, 2006), No. 5, pp. 119–161 [in Russian].